Nuclear Magnetic Resonance Investigation of the Cytochrome Oxidase–Phospholipid Interaction: A New Model for Boundary Lipid†

S. Y. Kang, H. S. Gutowsky, J. C. Hsung, Russell Jacobs,‡ Tsoo E. King, David Rice,§ and Eric Oldfield*

ABSTRACT: Deuterium nuclear magnetic resonance spectra of 1-myristoyl-2-[14′,14′,14′-$^2H_3$]myristoylphosphatidylcholine (DMPC-d_3), 1,2-[16′,16′,16′-$^2H_3$]dipalmitoylphosphatidylcholine (DPPC-d_6), 1-[16′,16′,16′-$^2H_3$]palmitoyl-2-palmitoleylphosphatidylcholine (PPPC-d_3), and 1-myristoyl-2-[6′,6′-$^2H_2$]myristoylphosphatidylcholine [DMPC-2-(6′,6′-d_2)] have been obtained in the presence of cytochrome oxidase (ferrocytochrome c:O_2 oxidoreductase, EC 1.9.3.1) as a function of temperature and composition and for the pure lipid as a function of temperature by using the quadrupole-echo Fourier transform method at 34.1 MHz. Above T_c, the temperature of the gel-to-liquid crystal phase transition of the pure phospholipid, all of the spectra have a single quadrupole splitting with no evidence of a second component. For DMPC-d_3 the splitting at ~30 °C decreases monotonically with cytochrome oxidase concentration from ~3.7 kHz in the pure lipid to ~2.6 kHz at 90 wt % protein. Plots of quadrupole splitting vs. protein–lipid ratio are linear, indicating that a simple two-site exchange model may be sufficient to account for the results observed. This shows that the methyl groups are "less ordered" in the "boundary lipid" than in the free lipid bilayer. Moreover, the exchange between the two sites is fast enough ($>10^3$ s^{-1}) to average out their 1-kHz difference in splitting. Similar, less extensive results were obtained for the other methyl-labeled lipids. However, DMPC-2-(6′,6′-d_2) with 67 wt % cytochrome oxidase has a spectrum with somewhat broadened features but with about the same splitting (28 kHz) as the pure lipid. Thus, the 6′-CH_2 group not only is more ordered in the pure lipid than the terminal methyl group but also its order parameter is less affected by the protein. In lipid samples containing cytochrome oxidase, the exchange-averaging and increased disorder of the terminal methyl groups persist immediately below T_c. But as the temperature is lowered further, a broad gellike component with a splitting of ~15 kHz develops in addition to the narrow component (~3-kHz splitting) from the boundary lipid associated with the protein. So the exchange has become too slow to average out the 10-kHz difference in splitting. The greater disorder of the terminal methyl groups in the boundary lipid both above and below T_c is compared with spin-label data interpretations which have suggested that the boundary lipid is more ordered. It is suggested that the motions of the hydrocarbon chains in boundary lipid may be more random and of larger amplitude, though slower, than in pure lipid bilayers. Many of the spectra have features less sharp than those of the theoretical powder pattern. They were analyzed by using simulation techniques with several possible mechanisms for broadening the transitions. Two were found to be important under various circumstances—a Lorentzian broadening derived from the decay rate T_{2e} of the quadrupole echo and a Gaussian distribution of order parameters.

In the past 10 years there has been considerable interest in applying "physical" techniques, such as scanning calorimetry, electron spin resonance (ESR),[1] neutron diffraction, Raman spectroscopy, nuclear magnetic resonance (NMR) spectroscopy, X-ray diffraction, and fluorescence spectroscopy, to study the structure of cell membranes [see, for example, Oldfield et al. (1978a) and references cited therein]. It is hoped that a better understanding of membrane structure will eventually lead to a better understanding of membrane function. A principal conclusion of these studies is that most membranes consist of a lipid bilayer which in many but not all instances may be "fluid" (Singer & Nicolson, 1972; Oldfield, 1973) and that the hydrophobic segments of membrane proteins penetrate the lipid bilayer. This anchors the protein, which may contain some sort of receptor such as the MN antigen (Segrest et al., 1974; Tomita & Marchesi, 1975) or be involved in say mitochondrial electron transfer (King, 1977) or ion transport (Warren et al., 1974).

It is quite generally thought that one of the effects of protein incorporation is to cause a special "ordered" or "immobilized" class of lipid molecules which are in intimate contact with the protein surface, the so-called "boundary lipid" (Jost et al., 1973a; Marsh et al., 1978) or annulus (Warren et al., 1974, 1975; Hesketh et al., 1976). A large number of studies, using the spin-label technique, have revealed such boundary lipids in systems as diverse as cytochrome oxidase (EC 1.9.3.1), sarcoplasmic reticulum (SR) ATPase (EC 3.6.1.3), gramicidin

† From the Department of Chemistry, University of Illinois at Urbana–Champaign, Urbana, Illinois 61801 (S.Y.K., H.S.G., R.J., D.R., and E.O.), and Department of Chemistry and the Laboratory for Bioenergetics, State University of New York at Albany, Albany, New York 12222 (J.C.H. and T.E.K.). *Received December 6, 1978.* This work was supported by the National Science Foundation (Grant PCM 76-01491 to E.O. and CHE 77-04585 to H.S.G), by the National Institutes of Health (Grant HL-19481 to E.O., HL-12576 and GM-16767 to T.E.K.), by the American Heart Association with funds provided in part by the Illinois Heart Association (Grant 77-1004 to E.O.), by the Illinois Heart Association (Grant N-6 to E.O.), by the Heart Association of Eastern New York, Inc. (T.E.K.), and by the Alfred P. Sloan Foundation (E.O.).

* Alfred P. Sloan Research Fellow, 1978–1980.

‡ Supported by a Fellowship from the Illinois Heart Association.

§ Supported by a U.S. National Institutes of Health, Cell and Molecular Biology Training Grant (Grant GM-07283).

[1] Abbreviations used: DMPC, 1,2-dimyristoyl-3-*sn*-phosphatidylcholine; DPPC, 1,2-dipalmitoyl-3-*sn*-phosphatidylcholine; PPPC, 1-palmitoyl-2-palmitoleyl-3-*sn*-phosphatidylcholine; NMR, nuclear magnetic resonance; ESR, electron spin resonance; TLC, thin-layer chromatography; SR, sarcoplasmic reticulum.

0006-2960/79/0418-3257$01.00/0

A′ (Chapman et al., 1977), and cytochrome b_5 (Dehlinger et al., 1974). In addition, recent NMR investigations (Longmuir et al., 1977; Dahlquist et al., 1977) have appeared to support the idea of a rigid, ordered boundary lipid in the cytochrome oxidase–phospholipid system.

Conventional thought then is that the fluid mosaic model gives a generally correct view of membrane organization and that the boundary lipid hypothesis gives a more detailed picture of the microscopic interactions occurring between the major membrane components—the lipids and proteins. However, the information obtained to date on the nature of such protein–lipid interactions at the molecular level is very limited. Since many membrane-bound enzymes, e.g., the SR ATPase, cytochrome oxidase, pyruvate oxidase, and β-hydroxybutyrate dehydrogenase, are activated by lipids [see, for example, Gennis & Jonas (1977)], it seems worthwhile to further characterize the nature of the protein–lipid associations.

Deuterium NMR of labeled lipids provides an essentially nonperturbing probe of molecular motion in both model and biological membranes (Oldfield et al., 1971, 1972, 1976, 1978a,b,c; Charvolin et al., 1973; Seelig & Seelig, 1974; Davis et al., 1976; Seelig, 1977; Mantsch et al., 1977; Stockton et al., 1976). There is the added bonus that Raman scattering and neutron diffraction experiments, which utilize the different scattering properties of ^2H over ^1H, may often be carried out on the same samples as used for the NMR experiments.

We have recently reported (Oldfield et al., 1978c) preliminary ^2H NMR studies of the interaction of a variety of proteins with the ^2H-labeled phosphatidylcholines 1-myristoyl-2-[14′,14′,14′-$^2H_3$]myristoylphosphatidylcholine (DMPC-d_3) and 1-[16′,16′,16′-$^2H_3$]palmitoyl-2-palmitoleylphosphatidylcholine (PPPC-d_3). The results indicate, at least as viewed by the terminal methyl group, that protein (or polypeptide) in general disorders the boundary lipid. In this paper we present additional results on the effects of cytochrome oxidase (cytochrome c:O_2 oxidoreductase, EC 1.9.3.1) on hydrocarbon chain mobility in ^2H-labeled DMPC, PPPC, and dipalmitoylphosphatidylcholine (DPPC) as a function of lipid–protein complex composition and temperature. We compare these results with those obtained by using the ESR spin-label technique (Jost et al., 1973a,b; Marsh et al., 1978) and discuss the apparent differences in conclusions reached about the state of boundary lipid when these two different spectroscopic techniques are used. In the following paper, we present ^2H NMR spectra of ^2H-labeled *Escherichia coli* cell membranes which support the presence of disordered boundary lipid in an intact biological membrane (Kang et al., 1979). In the third paper in this issue we present more detailed ^2H NMR results obtained on a simple model system—the lecithin–gramicidin A′ system (Rice & Oldfield, 1979). In all instances we emphasize the importance of time scale differences between the EPR and NMR experiments.

Experimental Section

Nuclear Magnetic Resonance Spectroscopy

Materials and Methods. Deuterium Fourier transform NMR spectra were obtained at 34.1 MHz (corresponding to a magnetic field strength of 5.2 T) by using the quadrupole-echo pulse technique (Davis et al., 1976). The "home-built" high-field NMR spectrometer described previously was used for data acquisition (Oldfield et al., 1978a). We used single-phase detection and a spectrum reverse technique (Nicolet software package FT-74) to obtain an effective 100-kHz spectral width. The spectrometer zero frequency was established by using a sample of hexadecanoic-*16,16,16-d*$_3$ acid dissolved in $CHCl_3$. Spectral phase corrections used were those which gave the best fit of the experimental spectrum to the theoretical ^2H powder pattern (see below). The 90° pulse width was 6–7 μs, which is adequate power for the ^2H spectra in all of the systems investigated. T_{2e} values were determined by using both integrated intensities of Fourier transformed spectra and peak intensities.

Spectral Simulations. Spectral simulations were carried out on the University of Illinois Digital Computer Laboratory's Control Data Corporation Cyber-175 system, which is interfaced to a Tektronix 4006 graphics terminal and interactive digital plotter (Tektronix, Beaverton, OR) in our laboratory. NMR data manipulation was performed on a Nicolet 1083 12K × 20 bit machine (Nicolet Instrument Corp., Madison, WI).

Synthesis of Deuterium-Labeled Phospholipids. ^2H-Labeled DMPCs were from the batch whose synthesis has already been described in detail (Oldfield et al., 1978a). 1,2-[16′,16′,16′-$^2H_3$]DPPC was synthesized by using basically the acylation technique of Khorana (Gupta et al., 1977). Hexadecanoic acid labeled in the terminal methyl group was synthesized by Kolbe electrolysis of acetic-d_3 acid (Merck, Sharp and Dohme, Montreal, Canada) and 1-methyl hexadecane-1,16-dioate (methyl thapsate), which was prepared from thapsic acid (Aldrich Chemical Co., Milwaukee, WI) by using the methylation–$Ba(OH)_2$ method (Durham et al., 1963). The monomethyl thapsate was purified by column chromatography on Merck silica gel 60 (Brinkmann Instruments, Des Plaines, IL) by using $CHCl_3$ as eluant, prior to electrolysis. The DPPC-d_6 prepared by the Khorana method was purified by column chromatography on silica gel 60 by using 2.3:1 $CHCl_3$–MeOH (v/v) as eluant.

Synthesis of the ^2H-labeled unsaturated phospholipid 1-[16′,16′,16′-$^2H_3$]palmitoyl-2-palmitoleylphosphatidylcholine was carried out by clipping the 2-chain of the DPPC-d_6 with phospholipase A_2 (snake venom of *Crotaleus adamateus*; Sigma Chemical Co., St. Louis, MO) as described previously (Oldfield et al., 1978a), followed by reacylation with palmitoleic anhydride with 4-(dimethylamino)pyridine as catalyst (Gupta et al., 1977). Palmitoleic anhydride was prepared from palmitoleic acid (*cis*-hexadec-9-en-1-oic acid; Sigma Chemical Co., St. Louis, MO) by using dicyclohexylcarbodiimide (Selinger & Lapidot, 1966). All manipulations were carried out under N_2.

Phospholipid purity was verified by thin-layer chromatography (TLC) on Merck silica gel 60 F-254 plates (EM Laboratories, Inc., Elmsford, NY), using in most cases a $CHCl_3$–MeOH–7 M NH_4OH (230:90:15, v/v) solvent system. Visualization was with one or more of the following reagents: I_2, rhodamine 6G, molybdenum phosphate reagent (Dittmer & Lester, 1964), or Dragendorff choline reagent (Bregoff et al., 1953). Phospholipid purity was also checked periodically during a given series of NMR experiments, and without fail on each and every sample after NMR spectroscopy. In the latter cases, samples were freeze-dried and then extracted with $CHCl_3$–MeOH (2:1, v/v). For the microsamples required for TLC, this process took less than 1 h/sample. During our studies we have found such checks to be absolutely essential since in several instances sample breakdown occurred (to phosphatidic acid and diglycerides and to lysolecithin), especially when protein is incorporated into the lipid bilayer. Furthermore, the products usually affect the spectra observed.

Protein Isolation and Protein–Lipid Reconstitution. Cytochrome *c* oxidase (cytochrome c:O_2 oxidoreductase, EC 1.9.3.1) was isolated from fresh beef hearts by using the

procedure of Yu et al. (1975) and Hartzell et al. (1978) with minor modifications. The method involves the sequential fractionation of the respiratory chain from the Keilin–Hartree preparation (King, 1967). It produces cytochrome oxidase from which more than 99.5% of the endogenous lipid is removed. Formation of cytochrome oxidase–^{2}H-labeled lipid complexes was carried out by using a cholate dialysis method (Dahlquist et al., 1977) in which samples were dialyzed for 72 h over Amberlite XAD-2 resin (British Drug Houses, Poole, Dorset, England) to ensure complete removal of cholate (Hesketh et al., 1976).

Cholate removal was verified on some samples by using [^{3}H]cholate (New England Nuclear, Boston, MA). Lipid phosphorus was determined by using the method of Ames & Dubin (1960), and protein concentration was determined by using the method of Lowry et al. (1951). Enzyme activity was assayed by using published methods (Kuboyama et al., 1972; Yu et al., 1975; Hartzell et al., 1978). Samples for NMR spectroscopy were dialyzed against ^{2}H-depleted H_2O (Aldrich Chemical Co., Milwaukee, WI) and then concentrated by ultracentrifugation. Typically, they contained 10–20 mg of phosphatidylcholine in ~200 μL of deuterium-depleted water.

Electron Spin Resonance Spectroscopy

One sample of DMPC–cytochrome oxidase was examined by using the spin label 16-NS [2-(14-carboxytetradecyl)-2-ethyl-4,4-dimethyl-3-oxazolidinyloxy], which was provided by Professor R. B. Gennis and had been purchased from Syva Associates (Palo Alto, CA). Complexation with DMPC–cytochrome oxidase was carried out basically as described by Jost et al. (1973a), and ESR spectra were obtained on a Varian E-3 spectrometer which operated at a fixed microwave frequency of ~9.5 GHz.

Results and Discussion

The theoretical background for the ^{2}H NMR spectra of lipid membranes is discussed in detail elsewhere (Oldfield et al., 1978a, and references cited therein; Seelig, 1977, and references cited therein). The principal result for the ^{2}H nucleus (with spin $I = 1$ and in C–D bonds an asymmetry parameter $\eta = 0$) is that the allowed transitions correspond to $+1 \leftrightarrow 0$ and $0 \leftrightarrow -1$ and give rise to a "quadrupole splitting" $\Delta\nu_Q$ of the NMR absorption lines (Figure 1A), where

$$\Delta\nu_Q = (3/4)(e^2qQ/h)(3\cos^2\theta - 1) \quad (1)$$

e^2qQ/h is the deuterium quadrupole coupling constant, which has been found to be ~170 kHz for C–D bonds (Derbyshire et al., 1969; Burnett & Muller, 1971), and θ is the angle between the principal axis of the electric field gradient tensor at the deuterium nucleus and the magnetic field H_0.

For a rigid polycrystalline solid all values of θ are possible and one obtains a so-called "powder pattern" line shape, Figure 1B, in which the separation between peak maxima is ~127.5 kHz and the separation between the outer "steps" is twice this value. In biological membranes, however, there is considerable motion of the C–D vector due, for example, to gauche–trans isomerization along the hydrocarbon chain, to methyl group rotation, to chain tilt, to diffusion, and to chain rotation. Thus, we must take an appropriate time average of $(3\cos^2\theta - 1)$ over the motions. For this purpose, we shall use the simple motional model of Petersen & Chan (1977). The vector and angle designations are shown in Figure 1C, where the director **d** is a laboratory fixed symmetry axis for a particular molecule, β is the angle between the C–D bond vector **r** and **d**, γ is the angle between the C–D bond vector and the instantaneous chain orientation **c** of the molecule, α is the angle between **c**

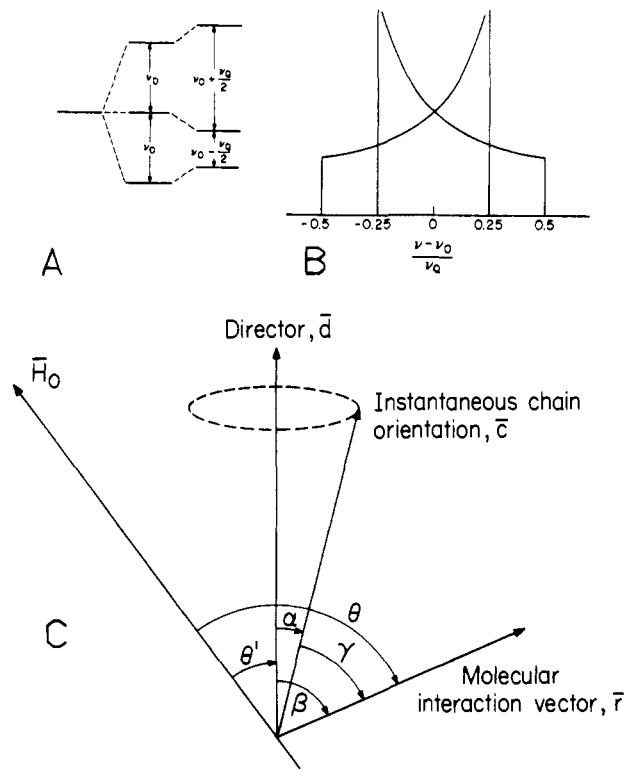

FIGURE 1: (A) Energy level diagram for spin $I = 1$ ^{2}H nucleus in a C–D bond in the presence of Zeeman and first-order quadrupolar interaction, assuming a zero symmetry parameter (axially symmetric electric field gradient). (B) Powder pattern line shape for ^{2}H nucleus in a rigid polycrystalline solid hydrocarbon. ν_Q is $3e^2qQ/2h$. (C) Angle and vector designations used in the text; from Petersen & Chan (1977).

and **d**, and θ' is the angle between **d** and H_0. The experimentally determined quadrupole splitting $\Delta\nu_Q$ may thus be written as eq 2 (Petersen & Chan, 1977; Oldfield et al., 1978a), where $\langle\ \rangle$ denotes an appropriate time average. The isotropic, static distribution in θ' for the usual "crystal powder" sample accounts for the experimental line shape, and the averaged quantities account for the splitting.

$$\Delta\nu_Q = (3/16)(e^2qQ/h)\langle 3\cos^2\alpha - 1\rangle\langle 3\cos^2\gamma - 1\rangle \times (3\cos^2\theta' - 1) \quad (2)$$

Theoretical Calculation of Experimental Spectra

All ^{2}H spectra we have observed have less "sharp" features than the theoretical ^{2}H powder pattern in Figure 1B, predicted by eq 2. That is, the transitions corresponding to a particular crystal orientation (θ') are broadened. Processes which may contribute to this broadening include ^{1}H–^{2}H dipolar interactions, ^{2}H quadrupolar relaxation, defect structures giving rise to a spread of quadrupole splittings, and exchange processes. The ^{1}H–^{2}H dipolar interactions are expected to be weak because of the small gyromagnetic ratio of deuterium and the relatively large ^{1}H–^{2}H distances. Indeed, it is found experimentally that high-power proton decoupling usually has a small effect on the appearance of ^{2}H powder spectra (R. A. Haberkorn and R. G. Griffin, private communication). The possible effects of the other three line broadening mechanisms are considered below in terms of the line shape function $g(\omega,\Delta\nu_Q)$. The variable ω is the resonance frequency relative to the central frequency ω_0.

Efficient quadrupole relaxation is expected to give a Lorentzian contribution to the ^{2}H NMR line width, leading to the line shape shown in eq 3, where δ is the half-width at half-height (HWHH) of the Lorentzian broadening function.

$$g(\omega,\Delta\nu_Q) = \int_0^{\pi/2} (d\theta \sin\theta)(\delta/\pi)/[\delta^2 + \{\omega \pm (\Delta\nu_Q/2) \times (3\cos^2\theta - 1)\}^2] \quad (3)$$

We have also tested a Gaussian broadening function, with a HWHH of $\Delta/2\ln 2$. In this case the line shape function is given by eq 4.

$$g(\omega,\Delta\nu_Q) = \int_0^{\pi/2} [(d\theta \sin\theta)/\Delta\sqrt{2\pi}] \exp[-\{\omega \pm (\Delta\nu_Q/2)(3\cos^2\theta - 1)\}^2/2\Delta^2] \quad (4)$$

A spread in quadrupole splittings might result from defects in the structure of the sample. For a Gaussian distribution in $\Delta\nu_Q$, centered about its mean value $\langle\Delta\nu_Q\rangle$, the line shape function becomes

$$g(\omega,\langle\Delta\nu_Q\rangle) = \sum_{\Delta\nu_Q} G(\Delta\nu_Q,\langle\Delta\nu_Q\rangle,\Omega)g(\omega,\Delta\nu_Q) \quad (5)$$

where

$$G(\Delta\nu_Q,\langle\Delta\nu_Q\rangle,\Omega) = (1/\Omega\sqrt{2\pi}) \exp[-(\Delta\nu_Q - \langle\Delta\nu_Q\rangle)^2/2\Omega^2] \quad (6)$$

and $\Omega/2\ln 2$ is the HWHH of the Gaussian distribution in $\Delta\nu_Q$.

The third broadening mechanism treated is the exchange of molecules between phases with different $\Delta\nu_Q$'s. For this case, we have assumed exchange between a quadrupole powder pattern, with splitting $\Delta\nu_Q$, and a narrow isotropic component at a rate such that the exchange broadening is proportional to ω^2. The result is very similar to eq 3 except that a Lorentzian broadening function is frequency dependent, that is

$$\delta = \delta_0 + c\omega^2 \quad (7)$$

where δ_0 is the broadening in the absence of the exchange and c is a constant.

We will now investigate whether or not our experimental ^{2}H NMR line shapes for the gel and liquid-crystalline ^{2}H-labeled bilayers may be analyzed in terms of these broadening functions. Heretofore, there have been only rather limited, semiquantitative analyses of ^{2}H spectral line shapes in bilayer membranes (Seelig, 1977; Dahlquist et al., 1977).

Comparison between Theory and Experiment for Model Systems

Fluid Liquid-Crystalline Phase. At 30 °C DMPC in excess water is in the fluid liquid-crystalline state (Chapman et al., 1967; Tardieu et al., 1973). We show in Figure 2D a ^{2}H NMR spectrum of DMPC labeled at the terminal methyl group of the 2-chain as CD_3, and in Figure 2B a spectrum of DMPC labeled as CD_2 in the 6′ position of the 2-chain is shown. Both spectra have the general shape expected for quadrupole splitting of a spin $I = 1$ nucleus and are consistent with a zero asymmetry parameter. Their doublet splittings indicate extensive motional averaging of the 128-kHz splitting for rigid C–D bonds. Moreover, the 3.6-kHz splitting for the CD_3 group (Figure 2D) is much less than the 29 kHz for the 6′-CD_2 group (Figure 2B), indicating that the terminal methyl group experiences more motional averaging than the CH_2 groups closer to the head group.

Both spectra lack the very sharp features due to the two singularities and the steps (or edges) of the powder distribution function (Figure 2A), suggesting that one or more of the line broadening mechanisms outlined in the preceding section is operative. In fact, very good agreement with the experimental line shapes in Figures 2B and 2D is obtained when the theoretical powder pattern is convoluted with a Lorentzian

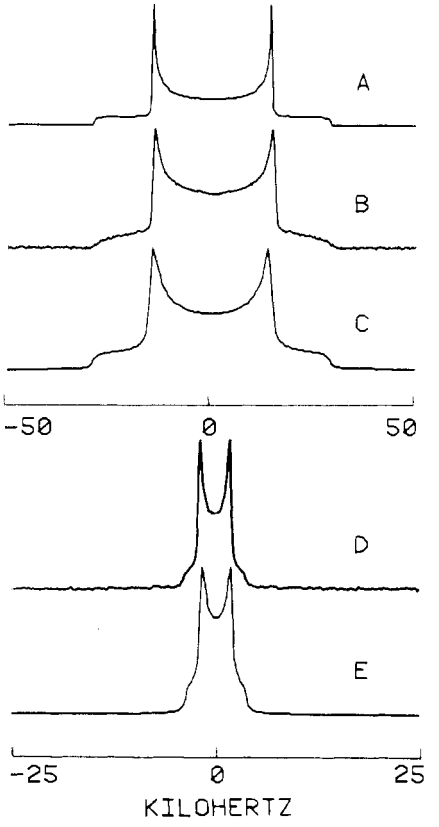

FIGURE 2: Experimental deuterium NMR spectra of DMPC-2-(*14′,14′,14′-d*$_3$) and DMPC-2-(*6′,6′-d*$_2$) bilayers in the liquid-crystalline state and some computer simulations. (See text, eq 3, for details of simulations.) (A) Simulated spectrum, $\Delta\nu_Q$ = 29 kHz, δ = 10 Hz. (B) DMPC-2-(*6′,6′-d*$_2$) in excess deuterium-depleted water, 30 °C, 100-kHz spectral width, 0.054-s recycle time, 10^4 scans, 2K data points, and $t_1 = t_2 = 40$ μs. (C) Simulated spectrum, $\Delta\nu_Q$ = 29 kHz, δ = 1.2 kHz. (D) DMPC-*d*$_3$ as in part B except 50-kHz spectral width, 0.54-s recycle time, and 6K scans. (E) Simulated spectrum, $\Delta\nu_Q$ = 3.6 kHz, δ = 290 Hz. The line widths used in the spectral simulations were obtained from the quadrupole-echo decay rate measurements, T_{2e}. Power falloff accounts for the decreased intensity in the wings of the spectrum of part B.

broadening corresponding to the measured decay of the quadrupolar echo, T_{2e}. For the sample of Figure 2B we have determined a T_{2e} of ~275 μs (Rice & Oldfield, 1979) corresponding to a broadening (δ) of 1.2 kHz, while for the sample of Figure 2D the T_{2e} is ~1.1 ms, a broadening of 290 Hz. Line shapes calculated with these broadenings and the observed splittings of 3.6 and 29 kHz are shown in Figures 2C and 2E, respectively. They are in excellent agreement with the experimentally determined line shapes. Gaussian broadenings do not improve the fit; neither does a Gaussian distribution of quadrupole splittings or a frequency-dependent line width, due to exchange processes (eq 7). The apparent discrepancy between 2B and 2C in the region of the step of the distribution function is due to an inadequate H_1.

By using measured T_{2e} values, we have obtained similar good agreement between experimental and calculated spectra for the gramicidin A′–lecithin system, even at very high gramicidin A′ concentrations where T_{2e} values of ~49 μs are obtained (Rice & Oldfield, 1979). This corresponds to about a 6-kHz broadening of the 28-kHz quadrupole splitting (Rice & Oldfield, 1979). Thus, the agreement shown in Figure 2 is not restricted to the relatively small broadening by T_{2e} in the pure liquid-crystal phase.

Crystalline Gel Phase. Below 23 °C DMPC in excess water exists in the so-called gel phase (Chapman et al., 1967; Tardieu et al., 1973). Below ~15 °C the Lβ' modification exists, and

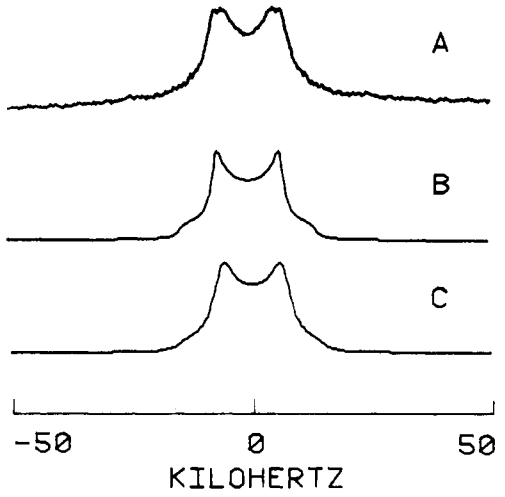

FIGURE 3: Comparison between experimental deuterium NMR spectrum of DMPC-d_3 in the gel state and various spectral simulations. (A) DMPC-d_3 in excess deuterium-depleted water, 18 °C (Pβ' phase), 100-kHz spectral width, 0.054-s recycle time, 4K data points, $t_1 = t_2 = 50$ μs, 6-μs 90° pulse widths, 10^4 scans, and 150-Hz line broadening. (B) Simulated spectrum with $\Delta\nu_Q = 14$ kHz using a Lorentzian line broadening (δ) of 1.8 kHz, corresponding to the measured T_{2e} of 186 μs. (C) Simulated spectrum using the Lorentzian broadening as in part B plus a Gaussian distribution of order parameters with a fractional width $\Gamma = 0.3$.

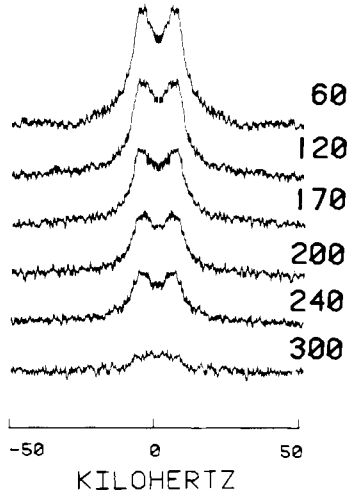

FIGURE 4: Partially relaxed spectra of DMPC-d_3 in the gel state (Pβ' phase) in excess deuterium-depleted water at 18 °C, 100-kHz spectral width, 0.54-s recycle time, 2K data points, 6-μs 90° pulse widths, 10^4 scans, and 150-Hz line broadening. The decay times ($2t$) are in microseconds. Least-squares analysis gives a T_{2e} value of 186 μs.

between 15 and 23 °C the Pβ' form exists (Chapman et al., 1967; Tardieu et al., 1973). We show in Figure 3A a ^{2}H NMR spectrum of DMPC-d_3 in excess water at 18 °C (Pβ' phase). In this phase, $\Delta\nu_Q$ is ~14 kHz, considerably larger than the 3.6 kHz of the more fluid liquid-crystalline phase. The experimental spectrum does not possess the sharp features of the theoretical powder pattern of Figures 1B and 2A, and proton decoupling has only a small effect on the line shape (R. A. Haberkorn and R. G. Griffin, private communication). We have determined the quadrupole-echo relaxation time T_{2e} for the sample as shown in Figure 4 and find it to be only 186 μs, indicating a Lorentzian broadening of ~1.8 kHz. The spectrum of Figure 3B, calculated with this broadening, is clearly much sharper than that of the experimental spectrum.

Earlier results suggest that the additional broadening may come from a distribution of quadrupole splittings about a mean value due to a rather disordered or "defective" structure of

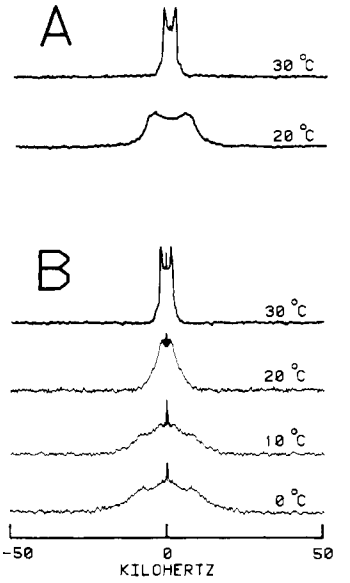

FIGURE 5: Deuterium NMR spectra of DMPC-d_3 bilayers containing cytochrome oxidase (ferrocytochrome c:O_2 oxidoreductase, EC 1.9.3.1) at *low* protein–lipid ratios as a function of temperature in excess deuterium-depleted water. (A) Pure DMPC-d_3. (B) DMPC-d_3 bilayer containing 60 ± 3 wt % cytochrome oxidase. Spectral conditions were typically 100-kHz spectral width, recycle time 0.54–2.4 s depending on the temperature, 4K data points, $t_1 = t_2 = 40$ μs, 6-μs 90° pulse width, 10^4 scans, and 150-Hz line broadening. Sample volume was ~200 μL.

the gel phase near the main thermal transition T_c. For example, vibrational Raman spectra indicate the presence of intramolecular disorder with some of the hydrocarbon chain in the gauche configuration rather than the all-trans configuration (Yellin & Levin, 1977); proton NMR results show, at least in sonicated vesicles, that fault dislocations may exist below T_c (Lawaczeck et al., 1976); and, in addition, spin-label partitioning experiments suggest the formation of defects in the lecithin gel phase, starting some 20 °C below the temperature of the main gel-to-liquid crystalline phase transition (Lee, 1977).

Figure 3C is a spectrum calculated with both the T_{2e} Lorentzian broadening function of 1.8 kHz and a Gaussian distribution of order parameters (quadrupole splittings) with a fractional width Γ of 0.3, where Γ is defined as in eq 8. This

$$\Gamma = \Omega/\langle\Delta\nu_Q\rangle \quad (8)$$

spectrum is in much better agreement with the experimental results. We have also investigated the possible importance of a frequency-dependent line width, due to exchange with an isotropic component, as in eq 7 (Loewenstein & Connor, 1963). However, this does not give as good a fit as the distribution of order parameters (Figure 3C).

Results on the Cytochrome Oxidase–Phospholipid Interaction

We have investigated the composition and temperature dependence of the interaction of lipid-depleted cytochrome oxidase (ferrocytochrome c:O_2 oxidoreductase, EC 1.9.3.1) with DMPC labeled at the terminal methyl position of the 2-chain and also the temperature dependence of this interaction for 2-[6,6-$^2H_2$]DMPC, 1-[16′,16′,16′-$^2H_3$]PPPC, and 1,2-[16′,16′,16′-$^2H_3$]DPPC. The results of these studies are presented in Figures 5–11. Preliminary work on DMPC-d_3 and PPPC-d_3 at high protein–lipid ratios has been reported previously (Oldfield et al., 1978c).

Interactions with DMPC-d_3. Experimental spectra are given in Figures 5A and 5B, respectively, for the pure lipid and for

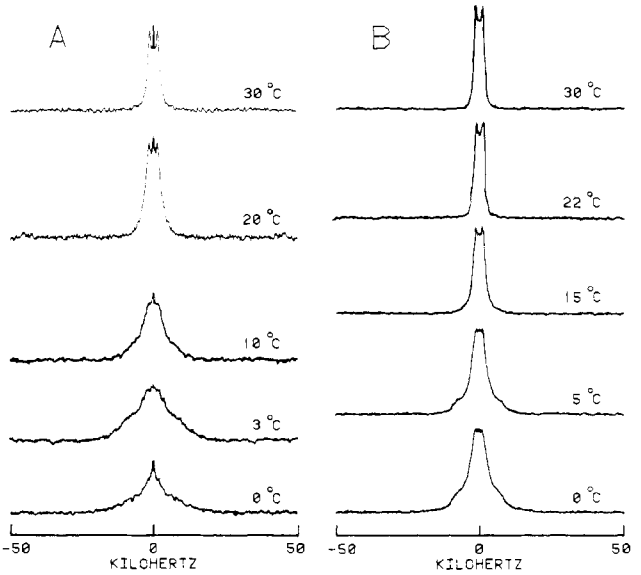

FIGURE 6: Deuterium NMR spectra of DMPC-d_3 bilayers containing cytochrome oxidase at *high* protein–lipid ratios as a function of temperature in excess deuterium-depleted water. (A) DMPC-d_3 bilayers containing 78 ± 4 wt % cytochrome oxidase. (B) DMPC-d_3 bilayers containing 85 ± 3 wt % cytochrome oxidase. Spectral conditions are as in Figure 5.

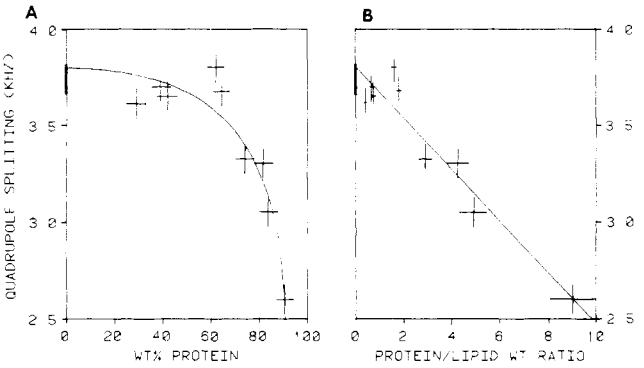

FIGURE 7: Graphs illustrating the effect of cytochrome oxidase on the ^{2}H NMR quadrupole splitting of DMPC-d_3 bilayers at 30 °C. (A) Graph of $\Delta\nu_Q$ vs. the weight fraction of protein. (B) Graph of $\Delta\nu_Q$ vs. the protein–lipid ratio (weight of protein/weight of lipid), illustrating two-site fast-exchange behavior. See the text for details.

lipid containing 60 ± 3 wt % of cytochrome oxidase, i.e., for low protein–lipid ratios, each at temperatures above and below 23 °C, the gel-to-liquid crystal transition temperature T_c of the pure lipid. Spectra under similar conditions are shown in Figures 6A and 6B for high protein–lipid ratios, 78 ± 3 and 85 ± 3 wt %. These results together with additional data (spectra not shown) are presented graphically in Figure 7A.

Above T_c the spectra for all of the samples are narrow doublets with no evidence of a second, boundary lipid component such as that reported for the PPPC-d_3 system (Dahlquist et al., 1977). The quadrupole splitting at ~30 °C is 3.7 ± 0.2 kHz for the pure lipid. However, the splitting decreases in proportion to the concentration of cytochrome oxidase, indicating that the protein decreases substantially the product of $\langle 3\cos^2\alpha - 1\rangle$ and $\langle 3\cos^2\gamma - 1\rangle$ in eq 2. To accomplish this the protein must cause at least some motions of the hydrocarbon chain in DMPC to be of greater amplitude and/or of higher frequency. In other words, the protein produces a large "disordering" of the lipid bilayer, at least in the region of the terminal methyl group of the lecithin 2-chain, in this disaturated C-14 species. These results indicate an "intrinsic" value for DMPC-d_3 boundary lipid of ~2.6 kHz; thus, the quadrupole splitting of the "bound" lipid is ~1 kHz less than that of the "free" lipid. The absence of any intermediate two-component spectra above T_c for any of the protein–lipid ratios investigated shows that there must be fast exchange between bound and free lipid at a rate in excess of 10^3 s^{-1} at these temperatures. The results of Figure 7A may be replotted in linear form by assuming a two-site fast-exchange model as follows. The observed quadrupole splitting ($\Delta\nu$) is related to the weight fractions of boundary lipid and free lipid by eq 9 or 10, where χ_b and χ_f are the weight

$$\Delta\nu = \chi_b\Delta\nu_b + \chi_f\Delta\nu_f \quad (9)$$

$$\Delta\nu = \chi_b(\Delta\nu_b - \Delta\nu_f) + \Delta\nu_f \quad (10)$$

fractions of boundary and free lipid and $\Delta\nu_b$ and $\Delta\nu_f$ are the quadrupole splittings of boundary and free lipid. If we assume that the weight fraction of boundary lipid is directly proportional to the amount of protein in the membrane, then

$$\chi_b = A(\text{protein/total lipid}) \quad (11)$$

or

$$\Delta\nu = A(\text{protein/total lipid})(\Delta\nu_b - \Delta\nu_f) + \Delta\nu_f \quad (12)$$

where A is a constant. We show in Figure 7B the results of plotting $\Delta\nu$ vs. the protein–lipid ratio (eq 12). The linear relation between $\Delta\nu$ and protein–lipid ratio supports a two-site fast-exchange model. It should in principle be possible to extract from such a plot the value of A, which is related to the amount of lipid which may form boundary lipid, and $\Delta\nu_b$, the quadrupole splitting of boundary lipid. However, at very high protein–lipid ratios residual cholate may exert a large influence on the lipid quadrupole splittings (D. Rice and E. Oldfield, unpublished experiments), reducing $\Delta\nu_b$. For example, we have found at ~3 wt % lipid that $\Delta\nu$ is only ~1.8 kHz. However, there is at least 1.5 wt % cholate bound in this case, i.e., the lipid–cholate ratio is ~2:1, and cholate has been found to greatly decrease the pure lipid $\Delta\nu_Q$ at this level (D. Rice, J. C. Hsung, T. E. King, and E. Oldfield, unpublished experiments). Previous studies of boundary lipid in the cytochrome oxidase system have suggested below ~15 wt % lipid that all lipid is associated with protein; therefore, we chose the value of 2.6 ± 0.2 kHz to be characteristic of this lipid. A value of ~2.4 ± 0.3 kHz may be estimated from our 3 wt % data after approximate correction for the effect of cholate.

These findings are not inconsistent with the observation of two sets of signals in the ESR experiment (Jost et al., 1973a,b). In order to get fast exchange behavior there, it would be necessary to have exchange rates on the order of the hyperfine coupling frequency, i.e., 10^8 s^{-1}. Lipid exchange has in fact recently been demonstrated by ESR spectroscopy (Jost et al., 1977), although it is yet to be substantiated that their results are indeed in quantitative agreement with the ^{2}H NMR limit on the lipid exchange rate.

On cooling of the pure lipid and sample containing 60 wt % protein ~5 °C below T_c, the spectra consist of broad, relatively featureless resonances (Figure 5). However, there is clearly a marked difference between the line shapes of the pure lipid and of the protein-containing bilayers. While the pure lipid gel-state line shape may be accurately simulated by using a Lorentzian broadening function and a Gaussian distribution of order parameters (splittings), the spectra of Figures 5B suggest that there are two main lipid environments in the presence of protein, each characterized by very different order parameters. Accurate determination of these two parameters is difficult, although it is clear that presence of the protein, even at relatively low concentration, induces formation of a more disordered membrane component. This is in fact

the behavior expected of an "impurity" molecule whose presence prevents chain crystallization and is, therefore, similar to that of cholesterol (Oldfield & Chapman, 1971, 1972; Oldfield et al., 1971, 1978a). A similar protein-mediated disordering effect has been suggested previously to explain ^{13}C NMR spectra for the sialoglycoprotein glycophorin interacting with a (head-group labeled) DPPC (Brûlet & McConnell, 1976).

Upon cooling of the samples with 78 and 85 wt % protein below T_c, a broad component appears with a line shape and width characteristic of the gel phase. This broad component is first clearly seen at about 10 (78 wt %) and 0 °C (85 wt %); it probably corresponds to molecules in free lipid bilayer regions which have crystallized. However, with the 85 wt % samples even at 0 °C, some 23 °C below T_c, there is clearly a sizable fraction of molecules characterized by a very narrow line width (Figure 6B). These signals must arise from lipid molecules which are associated with protein since the signal is largest and persists to the lowest temperatures in those samples containing the highest concentration of protein. This effect is not unique for cytochrome oxidase since rather similar effects have been noted previously for gramicidin A′, bacteriophage fl coat protein, myelin proteolipid apoprotein, and cytochrome b_5 (Oldfield et al., 1978c). The increased line width of the spectrum at 0 °C in Figure 6B is suggestive of a decrease in motion of the protein-associated lipid at low temperatures and/or of a wider distribution of quadrupole splittings in this heterogeneous system. In the absence of any data on protein being "squeezed" out of the bilayer by crystallization of the lipid hydrocarbon chains, or on the state of aggregation of the protein, a more detailed analysis of the low-temperature results will not be attempted at this time. The conclusions we draw from the data presented so far are that protein prevents chain crystallization below the T_c of pure lipid and above T_c it causes disordering of the hydrocarbon chains, as shown by the reduction in $\Delta\nu_Q$ of the terminal methyl group. Also above T_c, fast exchange ($>10^3$ s^{-1}) occurs between boundary and free lipid in the DMPC–cytochrome oxidase system.

Possible Effects of Residual Cholate. Protein–lipid complexes made by using detergent dilution and dialysis procedures inevitably contain residual quantities of detergent. For our cytochrome oxidase–lecithin complexes we typically reduced the cholate levels to 0.5 wt % of sample by extended dialysis over XAD-2 resin. However, it is important to establish whether or not these levels of cholate affect the deuterium quadrupole splittings, and, if so, in what way. Therefore, we have obtained spectra of DMPC-d_3 in the presence of controlled amounts of sodium cholate in the liquid-crystal phase at 30 °C as shown in Figure 8.

It is found that cholate *decreases* $\Delta\nu_Q$ (Figure 8A). The decrease in $\Delta\nu_Q$ is approximately linear with cholate concentration (Figure 8B). The cholate level observed in our oxidase–lipid complexes is shown by the vertical arrow. At these levels cholate has no appreciable effect on $\Delta\nu_Q$. Nonetheless, the general trend induced by cholate is the same as that of protein, so one must be cautious in interpreting spectra of protein–lipid recombinants prepared by detergent methods. It is noteworthy that the sample with 5 wt % cholate, although exhibiting a quadrupole splitting of ~3 kHz, was optically clear, in contrast to the normal opaque appearance of multilamellar lecithin vesicles.

Interactions with DPPC-d_6. The question now arises as to whether our results are representative only of a short, saturated, 2-chain labeled lecithin labeled in a terminal methyl

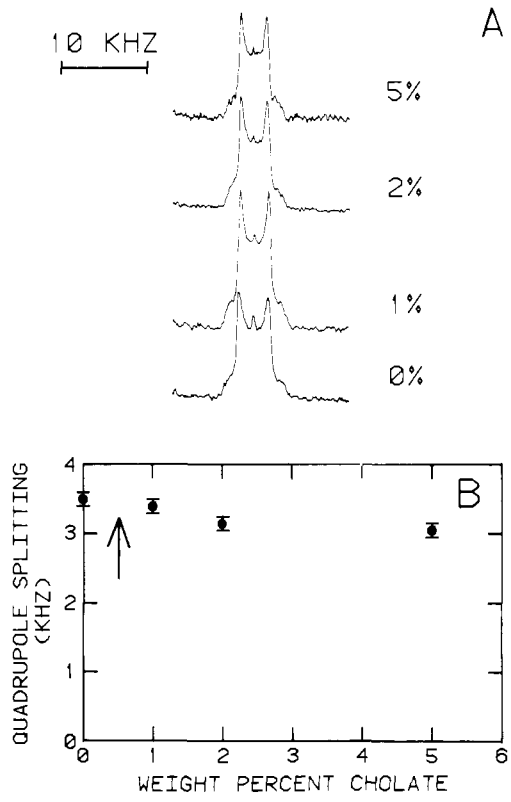

FIGURE 8: Deuterium NMR spectra of DMPC-d_3 bilayers containing cholate in excess deuterium-depleted water at 30 °C. (A) DMPC-d_3 plus cholate at the level indicated. Deuterium spectra were recorded by using a 50-kHz spectral width, 0.5–2-s recycle time, 4K data points, $t_1 = t_2 = 40$ μs, 6-μs 90° pulse widths, ~10^4 scans, and 100-Hz line broadening. (B) Graph of deuterium quadrupole splitting ($\Delta\nu_Q$) of DMPC-d_3 vs. the wt % cholate (data from part A). The arrow indicates the wt % cholate typically seen in our reconstituted protein–lipid complexes.

group. We chose this system for our initial studies of lipid membrane structure because of its low transition temperature (23 °C), which means that proteins will normally be in their native state when the lipid is in its liquid-crystalline phase, and because of the relative ease of synthesis and the oxidative stability of saturated vs. unsaturated lipids. The methyl label was used because of its small quadrupole splitting, even in the presence of cholesterol or in the crystalline gel state at liquid nitrogen temperatures (Oldfield et al., 1978a,c). This means that less radio frequency power is needed to obtain the undistorted ^2H NMR line shapes.

We present in Figure 9 results on a longer chain, disaturated species, DPPC-d_6, which again contains ^2H-labeled terminal methyl groups. The gel-to-liquid crystal phase transition temperature for DPPC is about 41 °C (Chapman et al., 1967). In the pure lipid below T_c (Figure 9A), the line shape and line width are similar to those obtained for DMPC-d_3 (Figure 3A), indicating that both chains crystallize. On decreasing the temperature, the spectra broaden, as for DMPC-d_3, reflecting a decrease in motion at the terminal methyl group of the hydrocarbon chain. This is consistent with the early ^1H NMR work of Veksli et al. (1969).

In the presence of 81 wt % cytochrome oxidase (Figure 9B), there is again a decrease in the quadrupole splitting of the terminal methyl group above T_c and a more dramatic effect below T_c, where a narrow line is observed down to ~10 °C. Two-component spectra are seen between 0 and 30 °C, which suggest but do not prove that the effects seen in Figure 6 are not simply due to our use of a rather short-chain species labeled only in the 2-chain. The results of Figure 9 (both C-16 chains

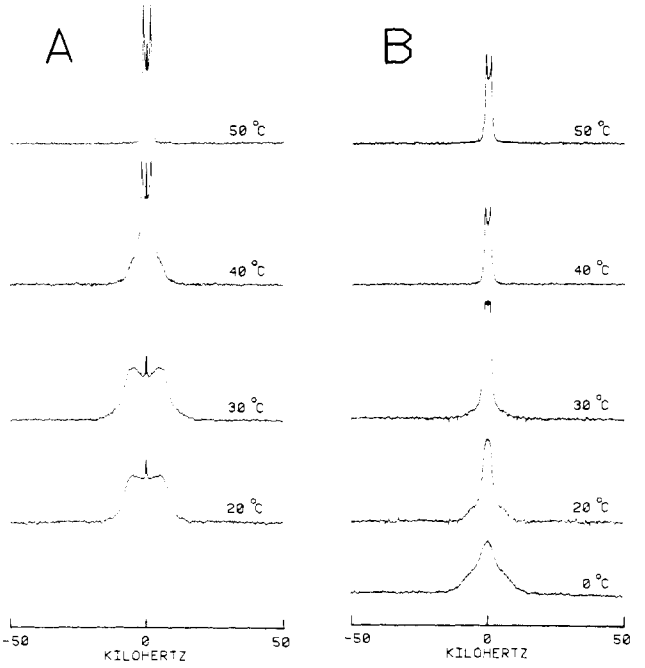

FIGURE 9: Deuterium NMR spectra of 1,2-[16′,16′,16′-$^2H_3$]DPPC (DPPC-d_6) bilayers in the absence and presence of cytochrome oxidase as a function of temperature in excess deuterium-depleted H_2O. (A) pure DPPC-d_6. (B) DPPC-d_6 sample containing 81 ± 3 wt % cytochrome oxidase. Spectral conditions were typically 100-kHz spectral width, 0.2–3.1-s recycle time depending on the temperature, 4K data points, $t_1 = t_2 = 40$ μs, 6-μs 90° pulse widths, and 150-Hz line broadening. The number of scans varied between 4K and 10K.

labeled) are completely consistent with those of Figure 6 (label only on the C-14 2-chain).

Interactions with PPPC-d_3. The question still arises as to whether the results presented so far are relevant to biological membranes, where the monounsaturated phospholipids, such as 1-palmitoyl-2-oleoylphosphatidylcholine, predominate. We therefore show in Figure 10 the results of experiments in which PPPC-d_3, the monounsaturated phospholipid 1-[16′,16′,-16′-$^2H_3$]palmitoyl-2-palmitoleylphosphatidylcholine (palmitoleyl is *cis*-hexadec-9-enoyl), has been complexed with lipid-depleted cytochrome oxidase by using the method of Dahlquist et al. (1977). The gel-to-liquid crystal phase transition of PPPC has been reported to be at about −15 °C (Dahlquist et al., 1977). At 30 °C, PPPC is thus some 45 °C above T_c, and the quadrupole splitting of the terminal methyl group is only ~2.0 ± 0.1 kHz (Figure 10A). This is close to the intrinsic boundary lipid value found for DMPC at 30 °C and is within experimental error the same as the 1.8 ± 0.1 kHz value found for the 74 wt % PPPC–cytochrome oxidase spectrum of Figure 10B at 30 °C.

At lower temperatures, however, there is a pronounced difference between the lipid and protein–lipid complex. At 0 °C the quadrupole splitting for the pure lipid is 3.1 ± 0.1 kHz (Figure 10A), while that for the 74 wt % protein–lipid complex is only 2.6 ± 0.1 kHz (Figure 10B). On further cooling to −20 °C, there is a continuous increase in spectral width for both labeled samples. Interestingly, there are no discontinuities apparent in $\Delta\nu_Q$ as the bulk water crystallizes to ice, even though it is likely that ice crystals penetrate the lipid bilayer (Siminovitch & Chapman, 1972). At −20 °C the pure lipid has undergone a phase transition to the gel state; however, the observed spectrum is still quite narrow, suggesting that the presence of the double bond causes a rather disordered gel phase. The effect of oxidase is thus far less dramatic than that for DMPC and DPPC.

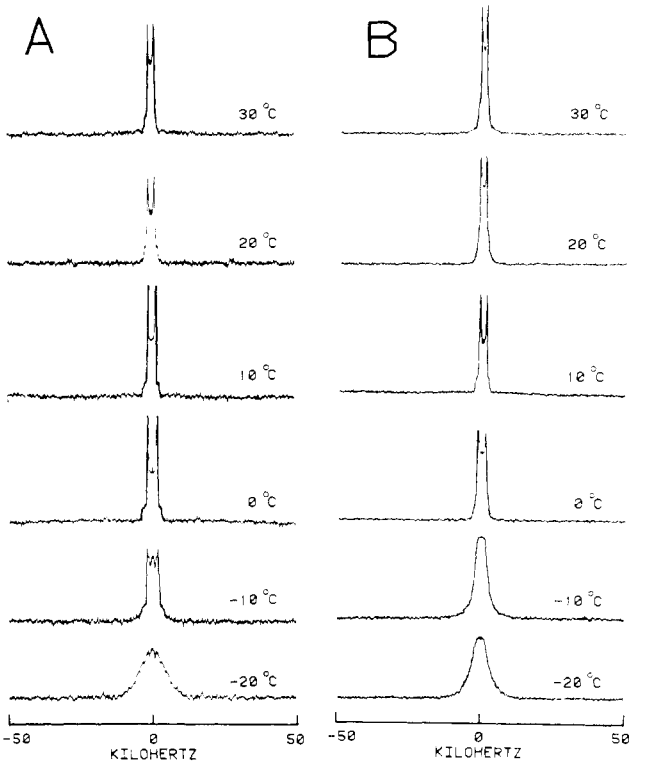

FIGURE 10: Deuterium NMR spectra of PPPC-d_3 bilayers in the absence and presence of 74 wt % cytochrome oxidase as a function of temperature in excess deuterium-depleted H_2O. (A) Pure PPPC-d_3. (B) PPPC-d_3 sample containing 74 ± 3 wt % cytochrome oxidase. Spectral conditions were typically 100-kHz spectral width, 0.5–3.1-s recycle time, 4K data points, $t_1 = t_2 = 50$ μs, 6-μs 90° pulse widths, 5K scans, and 150-Hz line broadening.

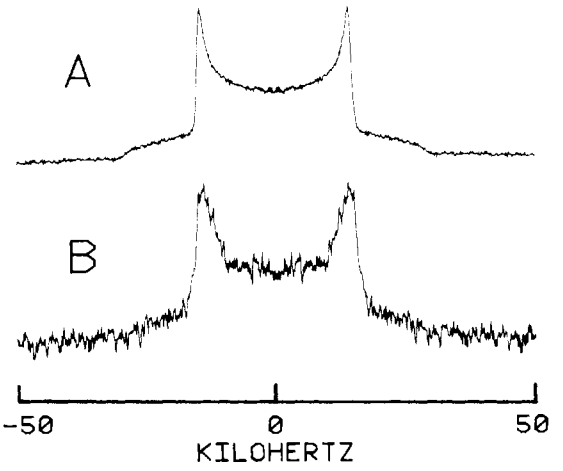

FIGURE 11: Deuterium NMR spectra of DMPC-2-(6′,6′-d_2) bilayers in the absence and presence of 67 ± 3 wt % cytochrome oxidase in excess deuterium-depleted water at 30 °C. (A) Pure DMPC-2-(6′,6′-d_2). (B) DMPC-2-(6′,6′-d_2) sample containing 67 ± 3 wt % cytochrome oxidase. Spectral conditions were 100-kHz spectral width, 0.31-s recycle time, 4K data points, $t_1 = t_2 = 40$ μs, 6-μs 90° pulse widths, 20K scans, and 200-Hz line broadening.

Interactions with DMPC-2-(6′,6′-d_2). From the results presented thus far, it appears that neither chain length, chain unsaturation, nor 1-chain/2-chain positions are critical factors for those features of protein–lipid association discussed above. There is, however, the possibility that the results for a terminal methyl group do not extend throughout the lipid chain. In addition, other lipids, such as the phosphatidylethanolamines, cerebrosides, sphingomyelins, etc., may have entirely different interactions with proteins, especially when the polar head-

groups contain charged residues. We have no experimental data on the latter point, but we have investigated the possibility that the effects we observe are restricted to the terminal methyl group (of a phosphatidylcholine).

In Figure 11 we present ^2H spectra for a sample of 1-myristoyl-2-[6′,6′-$^2H_2$]myristoylphosphatidylcholine in the absence and presence of ~67 wt % cytochrome oxidase. At 30 °C DMPC is in the liquid-crystalline phase, and a well-resolved quadrupole splitting $\Delta\nu_Q$ of ~28 kHz is obtained, Figure 11A (see also Figures 2B and 2C). In the presence of ~67 wt % cytochrome oxidase, the deuterium NMR spectrum of Figure 11B is obtained. It is seen that the magnitude of the quadrupole splitting $\Delta\nu_Q$ remains approximately the same as in the absence of protein (or is very slightly reduced), but the sharp features associated with the spectral singularity are broadened. Similar but more pronounced effects upon DMPC-2-(6′,6′-d_2) are observed when gramicidin A′ (Rice & Oldfield, 1979) or other proteins, e.g., the myelin proteolipid aproprotein (M. Meadows and E. Oldfield, unpublished experiments), are added.

Interpretation of the results for cytochrome oxidase is complicated by the fact that the 6′-methylene group in pure DMPC has a much larger splitting than the terminal methyl group. However, it is clear from the data of Figure 11 that the free and boundary lipids have rather similar splittings at the 6′ position. There is no "condensing" or ordering effect as found, for example, with cholesterol (Oldfield et al., 1971, 1978a,b), where $\Delta\nu_Q$ of DMPC-2-(6′,6′-d_2) increases from about 29 to 43 kHz upon addition of 20 mol % cholesterol and to ~55 kHz at 50 mol %.

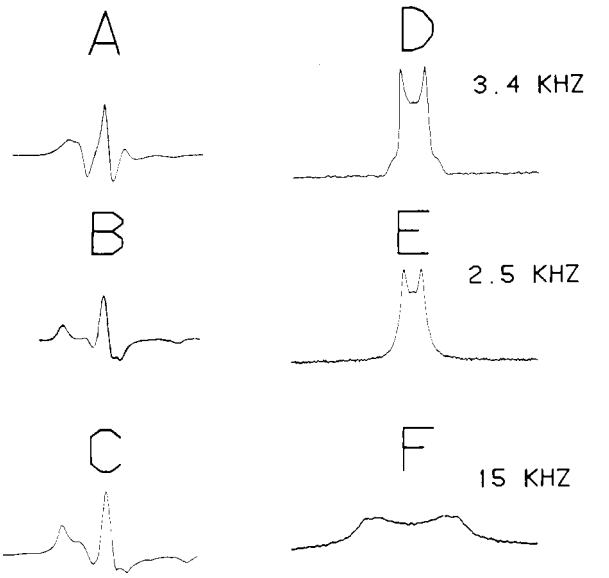

FIGURE 12: Comparison between ESR spin-label and deuterium NMR views (using a terminal methyl labeled lecithin) of hydrocarbon chain order in gel, liquid-crystal, and cytochrome oxidase–lipid (boundary lipid) states. ESR spectra: (A) 12-NS spin label in egg yolk lecithin liquid crystal at 20 °C [from Oldfield & Chapman (1971)]; (B) 14-NP spin label in cytochrome oxidase–boundary lipid [(from Jost et al. (1973b)]; (C) 12-NS in a DPPC gel at 20 °C [from Oldfield & Chapman (1971)]. Deuterium NMR spectra: (D) DMPC-d_3 in the liquid-crystalline phase at 30 °C [from Oldfield et al. (1978c)]; (E) DMPC-d_3 in a cytochrome oxidase–boundary lipid complex [from Oldfield et al. (1978c)]; (F) DMPC-d_3 in the gel state at −20 °C [from Oldfield et al. (1978c)].

Discussion

The results presented above indicate that cytochrome oxidase increases the disorder of lecithin hydrocarbon chains and prevents them from crystallizing into the gel phase below T_c, a cholesterol-like effect (Oldfield & Chapman, 1972). Above T_c it causes a disordering of the lipid hydrocarbon chains in the region of the terminal methyl groups for both saturated (C-14 and C-16) and unsaturated lecithins. In addition, the effects are not dependent on which chain is labeled. Above T_c the exchange between boundary lipid and free lipid must occur at a rate in excess of ~10^3 s^{-1} because only one averaged splitting is observed. Below T_c, where two-component spectra are observed, the exchange rate between boundary lipid (in the fluid state) and free gel-state lipid is too slow to average the two quadrupole splittings. It is not straightforward to place a limit on the exchange rate in this instance however since the domain sites are unknown.

The disordering effects are most pronounced at the terminal methyl end of the hydrocarbon chain. The effects, however, are a function of the protein or polypeptide incorporated into the bilayer. For example, gramicidin A′ causes a large decrease in $\Delta\nu_Q$ (and increased line broadening) as shown in the accompanying publication (Rice & Oldfield, 1979). These conclusions are reinforced by our recent ^{31}P NMR studies (S. Rajan, S. Y. Kang, H. S. Gutowsky, and E. Oldfield, unpublished experiments) in which we find that broadening of the ^{31}P resonance by chemical shielding anistropy ($\Delta\sigma$) is essentially the same in DMPC and in a DMPC–80 wt % oxidase complex, but $\Delta\sigma$ is collapsed and an isotropic line is observed for high gramicidin A′–lecithin complexes.

Although these results are not in agreement with those reported previously (Dahlquist et al., 1977; Longmuir et al., 1977), they are consistent with our previous findings for gramicidin A′, bacteriophage coat protein, myelin proteolipid apoprotein, and cytochrome b_5 (Oldfield et al., 1978c,). Thus, there may be significant differences between the cytochrome oxidase samples employed by the two groups. The variety of proteins and lipids and reconstitution techniques employed thus far in our studies is broad enough that our results may be representative of protein–lipid interactions as viewed by ^2H NMR spectroscopy. However, the NMR results apparently conflict with the rigid or ordered boundary lipid hypothesis put forward by Jost, Griffiths, and their co-workers on the basis of ESR spectra for spin labels attached to intermediate positions of the lipid chain (Jost et al., 1973a,b). The relationship between the NMR and ESR experiments is considered in the next section.

Comparison with the ESR View of Boundary Lipid. The parameters being motionally averaged in the ESR and ^2H NMR experiments are, respectively, the hyperfine and quadrupole interactions. The anisotropy of the hyperfine interaction $|A_{zz} - A_{xx}|$ is ~73 MHz. Thus, only motions having frequency components in excess of ~10^8 s^{-1} will affect the ESR spectrum; see, for example, Jost et al. (1971). For motional averaging of the ^2H quadrupole interaction the requirement is, however, that the rates involved be in excess of the ^2H quadrupole coupling, or $\gtrsim 10^5$ s^{-1}. Thereby, it is possible in principle to have motions fast enough to produce significant averaging of the quadrupole interaction [small order parameters; see, for example, Gaffney & McConnell (1974) and Seelig (1977)] but too slow to have much effect on a "rigid lattice" ESR spectrum.

In Figure 12 we present ESR spin-label and ^2H NMR results for lipid in three different states: lipid in a pure liquid-crystal bilayer, boundary lipid in a complex with cytochrome oxidase, and lipid in the crystalline gel state. It is immediately "seen" from Figure 12A–C that, as viewed by ESR, the lipid is most disordered (i.e., the hyperfine splitting is the least) in the liquid-crystal phase, while the rigid gel phase spectrum is similar in appearance to the boundary lipid in

cytochrome oxidase (Oldfield & Chapman, 1971; Jost et al., 1973a,b). However, as viewed by ^2H NMR, the terminal methyl group of boundary lipid is even more disordered (a smaller splitting) than in the liquid-crystal phase (Figures 12D,E), while the gel state is considerably more ordered than either (Figure 12F).

These results may all be explained as follows. The ESR spectrum of the spin-label 12-NS [methyl 12-(*N*-oxy-4′,4′-dimethyloxazolidinestearate)] in DPPC at 20 °C (Figure 12A) is characteristic of a nitroxide undergoing motions having a correlation time of $\sim 10^{-8}$ s (Itzkowitz, 1967), but the spectra of Figures 12B,C are near the rigid lattice limit; i.e., the correlation times of $\sim 8 \times 10^{-8}$ s (Itzkowitz, 1967) are too slow to cause much motional averaging. Thus, it is not easy to detect differences in these slow motions from the spectra of Figures 12B,C, although suitable techniques are available (Smigel et al., 1974). The motions occurring in the gel phase *could* be significantly slower, or involve completely different angular fluctuations, than the motions occurring in boundary lipid spin labels. However, the motions undergone by the spin labels are shown by the spectra of Figures 12B,C to be clearly of lower frequency than those undergone in the liquid-crystal phase (Figure 12A).

As discussed previously, the ^2H NMR results in this publication, and elsewhere (Oldfield et al., 1971), indicate that the gel state has significantly less motional averaging and is therefore more ordered than the liquid-crystalline state; see, for example, Figures 2 and 3. These results are consistent with the ESR results (Figures 12A,C) (Oldfield & Chapman, 1971). Nonetheless, the ^2H NMR results with the Me-labeled DMPC show that boundary lipid (Figure 12E) is more disordered than both the gel and liquid-crystalline states (Figures 12F,D), or as viewed by the 6′-labeled DMPC (Figure 11), the boundary lipid has approximately the same order. Thus, the apparent conflicts with the ESR data are greatest for the terminal methyl groups. Nevertheless, they may be reconciled by invoking the different rates of motion required for motional averaging in the ESR and ^2H NMR experiments and by considering the different types of motion that must be occurring in boundary lipid compared with those in the free lipid bilayer.

If the hydrocarbon chain motions in boundary lipid were simply slower than those in the liquid-crystalline phase, as suggested by Figures 12A,B, but were of the same angular distribution, then the quadrupole splitting of the boundary lipid (Figure 12E) would probably increase. This is not observed experimentally, and in fact the observed splittings either decrease or remain about the same on addition of protein to the lipid. For DMPC-d_3, the splitting decreases on addition of protein to pure lipid bilayers. This may be accomplished by averaging over larger angular displacements than in the liquid-crystal phase, the requirement for effective averaging being that the rate of the motions exceed $\sim 10^5$ s^{-1}.

Thus, on going from pure liquid-crystalline bilayer to boundary lipid the high-frequency oscillations may become slower, but these must be of increased amplitude (in θ). As a result, the motions are too slow ($<10^{-7}$ s) to affect the $(3 \cos^2 \theta - 1)$ angular factors that govern the hyperfine splitting of the ESR spectra. But in the ^2H NMR experiment, $(3 \cos^2 \theta - 1)$ decreases or remains about the same when one goes from the fluid liquid-crystalline phase to boundary lipid since the motions are still fast enough ($10^5 - 10^7$ s^{-1}) and have larger angular deviations. Boundary lipid is in motion and disordered on the ^2H NMR time scale, but relatively rigid as viewed by ESR. This "static" disordering of boundary lipid has been inferred previously by using ESR data (Jost et al., 1973a,b) where it was shown that in an oriented mixed bilayer lipid, boundary lipid system a rotation plot was obtained for the bilayer lipid but the boundary lipid spectrum did not change as a function of sample orientation in the magnetic field.

To account for these result, one needs a protein–lipid interaction that slows down motions of the lipid chain but enables at least some of the motions to increase in amplitude. This might come about by the selective interaction of the lipid head groups with the protein, which leaves the chains themselves more loosely packed. Thereby, the protein with its very irregular or rough surface (due to the presence of about 20 different amino acid side chains) in the lipid bilayer could facilitate isomerization of the lipid hydrocarbon chain by providing (time-dependent) vacancies at the protein–lipid interface, which in addition may arise from conformational fluctuations within the protein molecule itself and from protein rotation in the bilayer. According to this view, the motions of the terminal methyl groups would have the largest increase in amplitude (as found) while the center of the hydrocarbon chains and the head groups would be little affected. This agrees with our results (Figure 11) for DMPC-2-(6′,6′-d_2). Moreover, as viewed by the ^{31}P chemical shielding anistropy ($\Delta\sigma$), cytochrome oxidase has no ordering effect on the head-group region. The ^{31}P results suggest that the head-group organization of DMPC in the DMPC–cytochrome oxidase complex is similar to that in normal bilayer DMPC, although head-group motions are probably slower in the presence of protein.

The ^2H NMR picture of boundary lipid we have presented above was designed to be consistent with the ESR results. More work clearly needs to be done to clarify ^2H relaxation in these systems in terms of a more detailed motional model. Also, there is the question of whether specific interactions between the spin label and the protein itself could cause selective immobilization of the probe. For example, there might be hydrogen bonding between the spin-label N–O group and a peptide N–H residue, and such possibilities need to be investigated by using deuterated spin labels.

Implications of the Model. Our model for boundary lipid emphasizes the dynamically disordered nature of lipid associated with protein in a model bilayer membrane system and is to be contrasted with the static picture obtained from previous ESR studies. Boundary lipid is disordered, and in many instances may be exchanging with free bilayer lipid at rates in excess of 10^3 s^{-1}. We show in the following publication that protein–lipid interactions in an intact functional biological membrane, the cell membrane of *Escherichia coli* L48-2, have the same dynamic, disordered characteristics as in this model system (Kang et al., 1979).

Added in Proof

ESR results obtained by using a 12-NS labeled phospholipid spin label in DMPC (30 °C), DMPC oxidase (80% protein, 30 °C), and DMPC (18 °C) show essentially identically immobilized spectra for boundary lipid and gel-state systems (E. Oldfield and D. Rice, unpublished experiments).

References

Ames, B. N., & Dubin, D. T. (1960) *J. Biol. Chem. 235*, 769.
Bregoff, H. M., Roberts, E., & Delwiche, C. C. (1953) *J. Biol. Chem. 205*, 565.
Brûlet, P., & McConnell, H. M. (1976) *Biochem. Biophys. Res. Commun. 68*, 363.
Burnett, L. J., & Muller, B. H. (1971) *J. Chem. Phys. 55*, 5829.

Chapman, D., Williams, R. M., & Ladbrooke, B. D. (1967) *Chem. Phys. Lipids 1*, 445.
Chapman, D., Cornell, B. A., Eliasz, A. W., & Perry, A. (1977) *J. Mol. Biol. 113*, 517.
Charvolin, J., Manneville, P., & Deloche, B. (1973) *Chem. Phys. Lett. 23*, 345.
Dahlquist, F. W., Muchmore, D. C., Davis, J. H., & Bloom, M. (1977) *Proc. Natl. Acad. Sci. U.S.A. 74*, 5435.
Davis, J. H., Jeffrey, K. R., Bloom, M., Valic, M. L., & Higgs, T. P. (1976) *Chem. Phys. Lett. 42*, 390.
Dehlinger, P. J., Jost, P. C., & Griffith, O. H. (1974) *Proc. Natl. Acad. Sci. U.S.A. 71*, 2280.
Derbyshire, W., Gorvin, T., & Warner, D. (1969) *Mol. Phys. 17*, 401.
Dittmer, J. C., & Lester, R. L. (1964) *J. Lipid Res. 5*, 126.
Durham, L. J., McLeod, D. J., & Cason, J. (1963) *Organic Syntheses*, Collect. Vol. 4, p 635, Wiley, New York.
Gaffney, B. J., & McConnell, H. M. (1974) *J. Magn. Reson. 16*, 1.
Gennis, R. B., & Jonas, A. (1977) *Annu. Rev. Biophys. Bioeng. 6*, 195.
Gupta, C. M., Radhakrishnan, R., & Khorana, H. G. (1977) *Proc. Natl. Acad. Sci. U.S.A. 74*, 4315.
Hartzell, C. R., Beinert, H., van Gelder, B. F., & King, T. E. (1978) *Methods Enzymol. 53*, 54.
Hesketh, T. R., Smith, G. A., Houslay, M. D., McGill, K. A., Birdsall, N. J. M., Metcalfe, J. C., & Warren, G. B. (1976) *Biochemistry 15*, 4145.
Itzkowitz, M. S. (1967) *J. Chem. Phys. 46*, 3048.
Jost, P. C., Waggoner, A. S., & Griffith, O. H. (1971) in *Structure and Function of Biological Membranes* (Rothfield, L., Ed.) p 83, Academic Press, New York.
Jost, P. C., Griffith, O. H., Capaldi, R. A., & Vanderkooi, G. (1973a) *Proc. Natl. Acad. Sci. U.S.A. 70*, 480.
Jost, P. C., Griffith, O. H., Capaldi, R. A., & Vanderkooi, G. (1973b) *Biochim. Biophys. Acta 311*, 141.
Jost, P. C., Nadakavukaren, K. K., & Griffith, O. H. (1977) *Biochemistry 16*, 3110.
Kang, S. Y., Gutowsky, H. S., & Oldfield, E. (1979) *Biochemistry* (following paper in this issue).
King, T. E. (1967) *Methods Enzymol. 10*, 202.
King, T. E. (1977) *FEBS Symp. No. 45*, 17.
Kuboyama, M., Yong, F. C., & King, T. E. (1972) *J. Biol. Chem. 247*, 6375–6383.
Lawaczeck, R., Kainosho, M., & Chan, S. I. (1976) *Biochim. Biophys. Acta 443*, 313.
Lee, A. G. (1977) *Biochemistry 16*, 835.
Loewenstein, A., & Connor, T. M. (1963) *Ber. Bunsenges. Phys. Chem. 67*, 280.
Longmuir, K. J., Capaldi, R. A., & Dahliquist, F. W. (1977) *Biochemistry 16*, 5146.
Lowry, O. H., Roseborough, N. J., Farr, A. L., & Randall, R. J. (1951) *J. Biol. Chem. 193*, 265.
Mantsch, H. H., Saito, H., & Smith, I. C. P. (1977) *Prog. Nucl. Magn. Reson. Spectrosc. 11*, 211.
Marsh, D., Watts, A., Maschke, W., & Knowles, P. F. (1978) *Biochem. Biophys. Res. Commun. 81*, 397.
Oldfield, E. (1973) *Science 180*, 982.
Oldfield, E., & Chapman, D. (1971) *Biochem. Biophys. Res. Commun. 43*, 610.
Oldfield, E., & Chapman, D. (1972) *FEBS Lett. 23*, 285.
Oldfield, E., Chapman, D., & Derbyshire, W. (1971) *FEBS Lett. 16*, 102.
Oldfield, E., Chapman, D., & Derbyshire, W. (1972) *Chem. Phys. Lipids 9*, 69.
Oldfield, E., Meadows, M., & Glaser, M. (1976) *J. Biol. Chem. 251*, 6147.
Oldfield, E., Meadows, M., Rice, D., & Jacobs, R. (1978a) *Biochemistry 17*, 2727.
Oldfield, E., Glaser, M., Griffin, R., Haberkorn, R., Jacobs, R., Meadows, M., Rice, D., Skarjune, R., & Worcester, D. (1978b) in *Cellular Function and Molecular Structure. A Symposium on Biophysical Approaches to Biological Problems* (Agris, P. F., Loeppky, R. N., & Sykes, B. D., Eds.) p 55.
Oldfield, E., Gilmore, R., Glaser, M., Gutowsky, H. S., Hshung, J. C., Kang, S. Y., King, T. E., Meadows, M., & Rice, D. (1978c) *Proc. Natl. Acad. Sci. U.S.A. 75*, 4657.
Petersen, N. O., & Chan, S. I. (1977) *Biochemistry 16*, 2657.
Rice, D., & Oldfield, E. (1979) *Biochemistry* (third of four papers in this issue).
Seelig, J. (1977) *Q. Rev. Biophys. 10*, 353.
Seelig, A., & Seelig, J. (1974) *Biochemistry 13*, 4839.
Segrest, J. P., Gulik-Krzywicki, T., & Sardet, C. (1974) *Proc. Natl. Acad. Sci. U.S.A. 71*, 3294.
Selinger, Z., & Lapidot, Y. (1966) *J. Lipid Res. 7*, 174.
Siminovitch, D., & Chapman, D. (1971) *FEBS Lett. 16*, 207.
Singer, S. J., & Nicolson, G. L. (1972) *Science 175*, 720.
Smigel, M. D., Dalton, L. R., Hyde, J. S., & Dalton, L. A. (1974) *Proc. Natl. Acad. Sci. U.S.A. 71*, 1925.
Stockton, G. W., Polnaszek, C. F., Tulloch, A. P., Hasan, F., & Smith, I. C. P. (1976) *Biochemistry 15*, 954.
Tardieu, A., Luzzati, V., & Reman, F. C. (1973) *J. Mol. Biol. 75*, 711.
Tomita, M., & Marchesi, V. T. (1975) *Proc. Natl. Acad. Sci. U.S.A. 72*, 2964.
Veksli, Z., Salsbury, N. J., & Chapman, D. (1969) *Biochim. Biophys. Acta 183*, 434.
Warren, G. B., Toon, P. A., Birdsall, N. J. M., Lee, A. G., & Metcalfe, J. C. (1974) *Proc. Natl. Acad. Sci. U.S.A. 71*, 622.
Warren, G. B., Houslay, M. D., Metcalfe, J. C., & Birdsall, N. J. M. (1975) *Nature (London) 255*, 684.
Yellin, N., & Levin, I. W. (1977) *Biochemistry 16*, 642.
Yu, C-A., Yu, L., & King, T. E. (1975) *J. Biol. Chem. 250*, 1383.